International Journal on
"Technical and Physical Problems of Engineering"
(IJTPE)
Published by International Organization on TPE (IOTPE)

ISSN 2077-3528
IJTPE Journal
www.iotpe.com
ijtpe@iotpe.com

December 2010 | Issue 5 | Volume 2 | Number 4 | Pages 63-68

SOME ASPECTS ON CONTROL OF FUEL CELL HYBRID SOURCE AT THE FUEL CELL MAXIMUM POWER POINT UNDER DYNAMIC LOAD

N. Bizon

University of Pitesti, Pitesti, Romania, nicubizon@yahoo.com

Abstract- In this paper is analyzed a fuel cell Hybrid Power Source (HPS) topology that can operate at maximum power point of fuel cell stack. The HPS power topology and its control are simulated in Matlab - Simulink ® environment. The models for all used blocks are given and some control aspects are analyzed and discussed here.

Keywords: Hybrid Power Source, Maximum Power Point, Fuel Cell, Battery, Ultracapacitor, Modelling.

I. INTRODUCTION

As it is known, the fuel cell current dynamic must be limited in hybrid power source (HPS), especially when the Fuel Cell with Proton Exchange Membrane (PEMFC) is the main energy source of it. In the commercial PEMFC data sheet are mentioned some limitations for the level of PEMFC current regarding the ripple and slopes. These parameters are the main factors responsible for lower energy efficiency and reduced life cycle of PEMFC [1-6]. The level for the low frequency (LF) harmonics of PEMFC current set the PEMFC stack performances by hysteretic losses and more fuel consumption. Data sheet restrictions of the PEMFC ripple are specified on the frequencies bands and used in designing of the fuel cell HPS. The LF harmonics contributes with up to 10% reduction in the rated output power of PEMFC [7,8], so different solutions are proposed to mitigate of its [9-12]: increasing of the passive filter rated capacity, adding of active filters, implementing of an active control at the level of inverter system, using of interleaved converters, etc. For mono-phase inverter system powered by fuel cell HPS, the LF harmonics appear on high DC voltage bus at even multiples of twice of the grid frequency. For three-phase case, the LF harmonics appear at multiples of triple of grid frequency. These LF harmonics are propagated back through boost DC-DC converter on the HPS DC voltage bus. A HPS topology combines two or more energy sources and energy storage devices (ESD) that work together to supply the inverter system or store energy in ESD (such as stack of batteries and/or ultracapacitors) [13-16]. The HPS output port is a regulated DC voltage port [17]. The main control objective for the HPS vehicle applications is short respond to high energy demands [18-21]. When load require more power than is currently available from the PEMFC's stack, the bidirectional converter drains energy from those ESD in order to make up the lack (see Figure 1 adapted from [21]).

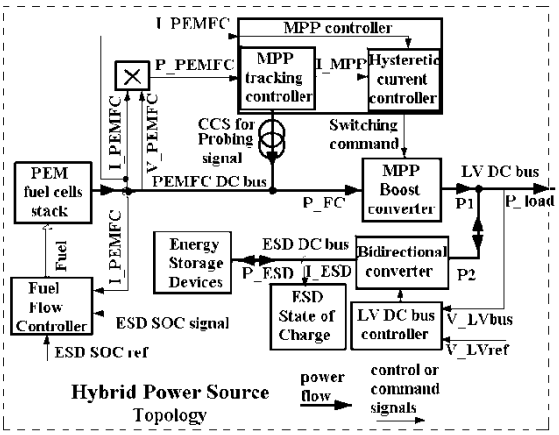

Figure 1. Hybrid power source topology

For high energy efficiency, in fuel cell HPS the PEMFC stack must operates in the region close to maximum power point (MPP) at rated fuel flow [22-25]. The fuel flow level is changed by fuel cell current if ESD state of charge (SOC) is in the admissible range. The PEMFC stack (P_{FC}) and ESD stack (P_{ESD}) assure the power flow on LV DC bus via the MPP boost converter (P_1) and bidirectional converter (P_2), respectively. The power balance is $P_{load}=P_1+P_2$, and the power management is assures by the MPP controller and LV DC bus controller. The fuel cell MPP current (I_{MPP}) is tracked in an adaptive feedback loop by injecting the probing current [26, 27]. The power ripple becomes lowest when the operation point gets closer to MPP [28]. Also, using of ultracapacitors as ESD in fuel cell-based vehicles permits reduction of the hydrogen consumption and a reliable PEMFC operating under sharp power pulses [29, 30, 31].

In this paper, the modelling analysis will be focused on operating control of the fuel cell HPS at MPP of PEMFC stack. The remainder of the paper is organized as follows. The analyzed HPS topology is shown in Section 2. Section 3 presents the proposed modelling of fuel cell HPS topology in the Matlab-Simulink® environment.

Section 4 shows the appropriate control of both HPS controllers: hysteretic current controller and MPP tracking controller. Section 5 shown representative simulation results and last section concludes the paper.

II. ANALYZED FUEL CELL HPS TOPOLOGY

In Figure 2 is shown the HPS topology that will be analyzed in this paper. Note that ESD are directly connected to the LV DC bus. Consequently, the voltage on LV DC bus will have a slow variation in order to assure the balance of power flows when the MPP is changed. This choice does not affect the MPP tracking process. In this case the power balance is $P_{load}=P_1+P_{ESD}$, where $P_{ESD}=P_{batt}+P_{Ucap}$.

The MPP boost converter is an appropriate solution to assure a low PEMFC current ripple. A hysteretic current controller is used to generate the switching command. The current error, I_{MPP}-I_{PEMFC}, is used to turn the switch on and off, resulting in free-running operation.

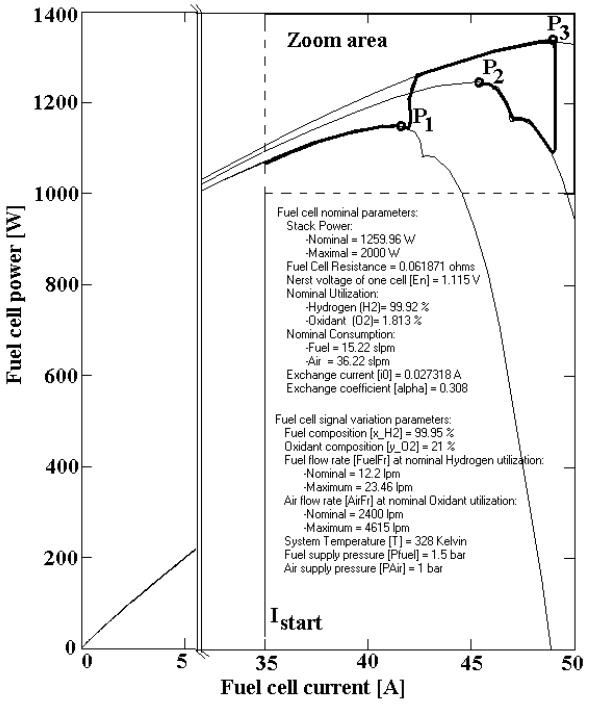

Figure 2. The MPP sequence for the 1.2 kW PEMFC stack

The load dynamic is simulated by the load sequence. The fuel flow controller is replaced with a MPP sequence that simulates the MPP changing in time as in Figure 3.

The dynamic of MPP in time must be tracked by MPP tracking controller in the adaptive feedback loop based on extremum seeking control (Figure 4). The probing signal is a sine wave, which is superimposed over the start current sequence (and this may be correlated with the start-up of PEMFC stack).

The parameters for Ballard Nexa PEMFC are shown in Table 1 at nominal fuel flow rate (12.2 lpm) [32], where V_{PEMFC0} is output voltage from no-load, V_{MPP} - output voltage, I_{MPPP} - output current, P_{MPP} - power, and $Z_{MPP} = V_{MPP}/I_{MPP}$.

Table 1. Base parameters for Ballard Nexa PEMFC

PEMFC stack	V_{PEMFC0} [V]	V_{MPP} [V]	I_{MPP} [A]	P_{MPP} [W]	Z_{MPP} [Ω]
Ballard Nexa	42,2	26,6	45	1200	0,59

The rated load power is $P_{load}=\eta_1 P_{MPP}$ considering $P_2\cong 0$. For $\eta_1\cong 90\%$ (where η_1 is the MPP boost converter efficiency) results the rated load power of $P_{load}\cong 1080W= V_{LVbus}\times I_{load}$. For example, if $I_{load}=10$ A, then $V_{LVbus}\cong 108V$. These levels are used in choosing of the proper ESD to assure the power balance.

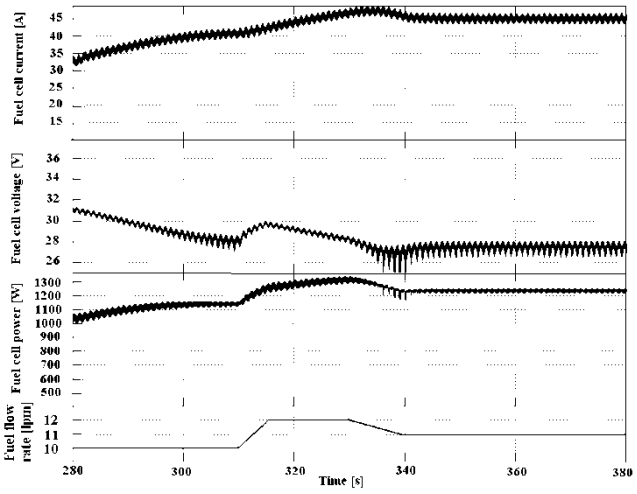

Figure 3. The tracking of the MPP sequence for 1.2 kW PEMFC stack

III. MODELLING OF FUEL CELL HPS

In this section, the used models for PEMFC stack, ESD stack and boost converter are briefly explained.

A. Model of PEMFC Stack

Many improvements have been made to fuel cell model in recent years [33, 34, 35]. The variation of the PEMFC temperature (T) in time (t) depends by fuel cell current (I_{FC}) and can be calculated as:

$$T = 273 + T_0 + \left(T_0 - T_{rt} + T_{ic}\cdot I_{FC}\right)\cdot\left(1-\exp\left(-\frac{t\cdot I_{FC}}{T_{it}}\right)\right) \quad (1)$$

where the parameters are mentioned in [36,37]. The hydrogen partial pressure can be obtained with:

$$p_{H2} = \frac{1/k_{H2}}{1+t_{H2}\cdot s}\left(Q_{H2}^{in} - 2\frac{N}{4FU}I_{FC}\right), t_{H2} = \frac{V_{anode}}{R\cdot T_{op}\cdot k_{H2}} \quad (2)$$

where t_{H2} is hydrogen time constant (s). Similarly, oxygen partial pressure can be obtained:

$$p_{O2} = \frac{1/k_{O2}}{1+t_{O2}\cdot s}\left(Q_{O2}^{in} - \frac{N}{4FU}I_{FC}\right), t_{O2} = \frac{V_{catode}}{R\cdot T_{op}\cdot k_{O2}} \quad (3)$$

where:

- t_{O2} is oxygen time constant (s);
- $V_{cathode}$ - Volume of the cathode (m^3);
- Q_{H2}^{in} - Oxygen input flow (kmol s^{-1} or l/min);
- k_{O2} - Oxygen valve molar constant [kmol (atm s)$^{-1}$];

Usually, the hydrogen and oxygen input flows are inputs for PEMFC model. The fuel flow rate is chosen as input parameter in this paper.

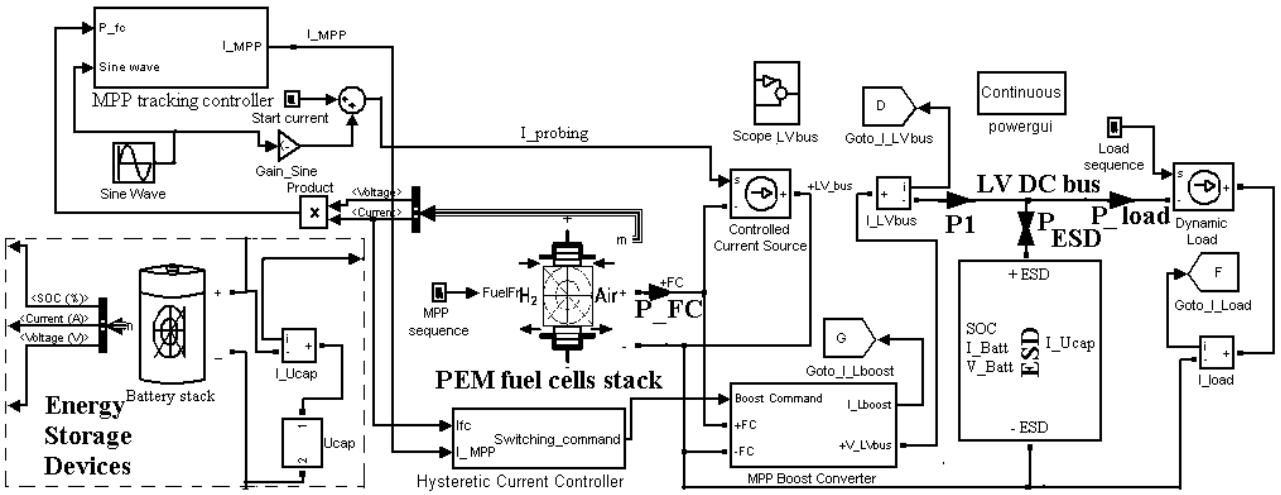

Figure 4. Analyzed fuel cell HPS topology (adapted from [21])

The Nernst's voltage is implemented as:

$$E_{Nerst} = 1.229 - 8.5 \cdot 10^{-4} \cdot (T - 298) + \\ + 4.308 \cdot 10^{-5} \cdot T \cdot \ln\left(P_{H2} + P_{O2}/2\right) \quad (4)$$

The activation voltage loss can be written as:

$$E_{act} = \xi_1 + \xi_2 \cdot T + \xi_3 \cdot T \cdot \ln(I_{FC}) + \xi_4 \cdot \ln(C_{O2}) \quad (5)$$

where C_{O2} represents the dissolved oxygen concentration in the interface of the cathode catalyst and the ξ_i parameters, i=1-4, are mentioned in references [33, 35, 36].

$$C_{O2} = \frac{P_{O2}}{5.08 \cdot 10^6 \cdot \exp\left(-498/T\right)} \quad (6)$$

The ohmic voltage loss is implemented as:

$$E_{ohmic} = J_{FC} \cdot R_{ohmic} \\ J_{FC} = I_{FC}/A;\ R_{ohmic} = R_m + R_c;\ R_m = r_m \cdot t_m / A \quad (7)$$

where:

R_{ohmic} is the ohmic resistance (Ω);
J_{FC} - Current density (A/cm^2);
R_m - Echivalent membrane resistance (Ω);
R_c - Contact resistance between membrane and electrodes (Ω);
t_m - membrane thickness [cm];
A - Activation aria (cm^2);
r_m - Resistivity of Nafion membrane (Ωcm^{2}m^{-1}):

$$r_m = \frac{181.6 \cdot \left[1 + 0.03 \cdot J_{FC} + 0.062 \cdot (J_{FC})^{2.5} \cdot \left(T/303\right)^2\right]}{\left[\lambda_m - 0.0634 - 3 \cdot J_{FC}\right] \cdot \exp\left[4.18 \cdot \left(T - 303/T\right)\right]} \quad (8)$$

where λ_m represent the water content of the membrane and it is a input of PEMFC model set to 2.

The concentration voltage loss is implemented in the subsystem 5 and can be written as:

$$V_{conc} = B \cdot \ln\left(1 - J_{FC}/J_{\max}\right) \quad (9)$$

where B is a modeling constant (V) and J_{max} represents the maximum current density (A/cm^2).

The PEMFC output voltage can be calculated as:

$$V_{FC} = N \cdot (E_{Nerst} - E_{ohmic} - V_d) \quad (10)$$

where V_d is voltage over R_a resistance and R_a is equivalent resistance representing the sum of activation and concentration resistances:

$$R_a = \frac{V_d}{I_{FC}} \frac{E_{act} + E_{conc}}{I_{FC}} \quad (11)$$

The PEMFC dynamic related to the R_a resistance in parallel with double layer capacitor (C) is implemented as:

$$I_{FC} = \frac{V_d}{R_a} + C \cdot \frac{d}{dt} V_d \Rightarrow V_d = \frac{I_{FC} \cdot R_a}{t_{FC} \cdot s + 1} \quad (12)$$

where t_{FC}=$C \cdot R_a$ represents the fuel cell time constant.

B. Model of Mixed ESD Stack

The used battery model in this paper is well known [38]. The exponential zone dynamics is modeled by:

$$E_{\exp}(q) = A \cdot \exp(-B \cdot q) \quad (13)$$

where:

q=$i_{batt} \cdot t$ is current battery capacity (Ah);
i_{batt} = Battery current (A);
A = Exponential voltage (V);
B = Exponential capacity (Ah)$^{-1}$.

Battery operating mode is modeled by S signal, which is the output of a comparison block that compare the low-pass filtered battery current, $i_{LPFbatt}$, with zero reference. Consequently, S = 0 during battery discharge ($i_{LPFbatt}$ >0) and S = 1 during battery charging ($i_{LPFbatt}$ <0). Finally, the battery voltage, E_{Batt}, is given by charge (f_c) or discharge (f_d) function as:

$$f_d(t) = E_W - K_r \frac{Q}{Q - q} \cdot i_{LPFbatt} - K_c \frac{Q}{Q - q} \cdot q + E_{\exp} \\ f_c(t) = E_W - K_r \frac{Q}{q + Q/10} \cdot i_{LPFbatt} - K_c \frac{Q}{Q - q} \cdot q + E_{\exp} \quad (14)$$

where:

E_w is a constant – the working battery voltage (V);
K_c = Polarization constant V/(Ah);
K_r = Polarization resistance (Ω);
$i_{LPFbatt}$ = Low frequency battery current dynamics (A);
Q = Maximum battery capacity (Ah).

Battery state of charge, SOC_{batt}, is computed as:

$$SOC_{batt} = 100 \cdot \left(1 - \int_0^t i_{batt} dt \Big/ Q \right) \quad (15)$$

The parameters for used 160V/38Ah battery are: A = 15V, B = 0.375(Ah)$^{-1}$, K_c = 0.03 V/(Ah), K_r = 0.03Ω, E_w = 163V, and Q = 43Ah. Internal resistance, r_{batt}, is set of 0.04 Ω and the battery output voltage, V_{batt}, is computed as:

$$V_{batt} = E_{batt} - r_{batt} \cdot i_{batt} \quad (16)$$

For the used 100F/160V ultracapacitors stack is used a first order model [35,36] with the series, R_s, and parallel, R_p, resistances set at 0.01 Ω and 1 kΩ, respectively.

C. Model of Boost Converter

The boost converter model is well known, so only the used parameters are given below. In on-state both IGBT and FW-Diode models have a R_{on} internal resistance and a L_{on} inductance of 0.01Ω and 1μH, respectively, but the forward voltage, V_F, is set different to 1V and 0.8V, respectively. Also, the fall time, T_f, and tail time, T_t, is set different to 1μs and 2μs, respectively. Both IGBT and FW-Diode models use a series RC snubber circuit with $C_{snubber}$=0.1μH and $R_{snubber}$ = 100Ω. The boost inductance, L_{boost}, is set to 10mH value and its series resistance, r_L, at 10mΩ.

IV. CONTROL OF FUEL CELL HPS

In this section, the HPS control is analyzed and briefly explained.

A. Hysteretic Current Controller

Switching command for boost converter is obtained using a hysteretic current controller (see Figure 5). The input current is the difference between the fuel cell current, i_{fc}, and the current output of the MPP tracking controller that estimate the MPP fuel cell current in an adaptive loop (see Figure 6).

The operating relationships of boost converter are

$$\begin{aligned} v_{FC} &= (r_L + R_{on}) \cdot i_{FC} + (L_{boost} + L_{on}) \frac{di_{FC}}{dt} + V_F \\ v_{FC} &= (r_L + R_{on}) \cdot i_{FC} + (L_{boost} + L_{on}) \frac{di_{FC}}{dt} + V_F + v_{LVbus} \end{aligned} \quad (17)$$

for IGBT on-state and FW-Diode on-state, respectively.

For example, at rated load and fuel cells stack operating at MPP ($V_{FC} = V_{MPP}$ = 26.6V, $I_{FC} = I_{MPP}$ = 45A) with a ripple factor of fuel cell current of about RF_{FC} = 5%, if V_{LVbus} = 100V, L_{boost} = 10mH, and neglecting the resistive effect in relationships (11), then switching period is $T \cong$ 1kHz (see relation 18):

$$T \cong (L_{boost} + L_{on}) \cdot RF_{FC} \cdot I_{MPP} \cdot \left(\frac{1}{V_{MPP}} + \frac{1}{V_{LVbus} - V_{MPP}} \right) \quad (18)$$

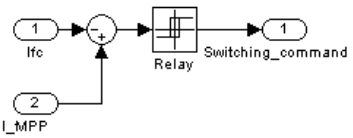

Figure 5. Hysteretic current controller of the boost converter

B. MPP Tracking Controller

The adaptive MPP feedback loop using a high-pass filter is explained in [26]. The advantages of using a band-pass filter centred on the sine frequency are shown in [39, 40]. After normalization of PEMFC power, P_{fc}, with k gain (=1/*Area*), the probing power signal is filtered and demodulated by multiplication with 1 Hz sine dither. After that, it is integrated and amplified by k_1 gain and, finally, is superimposed on it the amplified dither ($k_2 \sin \omega t$) (Figure 5). Some power spectrums are shown in next section. It is shown that only first three harmonics of probing power signal are important in the MPP tracking.

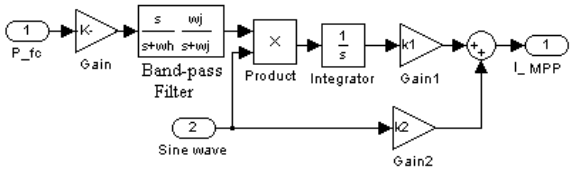

Figure 6. MPP tracking controller (adapted from [39])

V. SIMULATION RESULTS

The time for MMP tracking is around of hundreds of seconds when the start current is zero (Figure 3). In Figure 7 and 8 are shown the process of MPP tracking when the PEMFC operation (close of MPP) is perturbed by a pulse in the fuel flow rate (that gives $\Delta P \cong$ 500W). It can be observed that the time for MMP tracking is less of ten second. The PEMFC behaviour in the tracking of the MPP sequence shown in Figure 3 is presented in Figure 9. Without the bidirectional converter and its controller (see Figures 1 and 2), the voltage on the LV DC bus, V_{LVbus}, is around the ESD nominal voltage value to assure the power balance (see Figure 10).

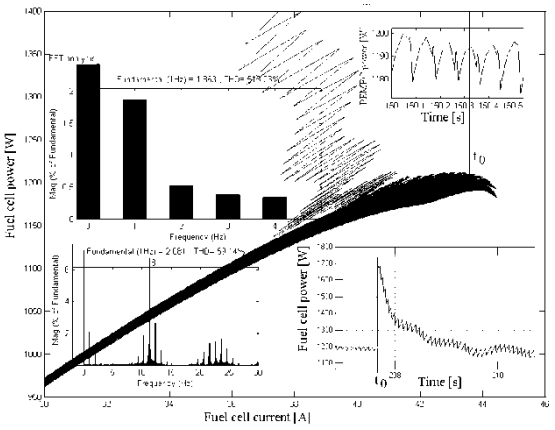

Figure 7. The MPP tracking in the P-I phase plane

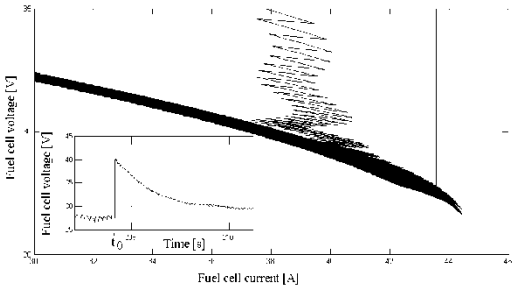

Figure 8. The MPP tracking in the U-I phase plane

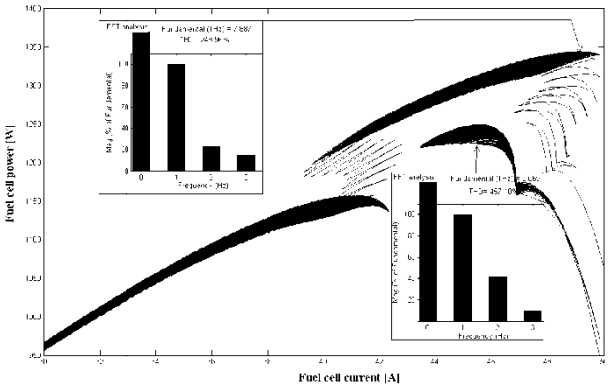

Figure 9. The PEMFC behaviour in the tracking of the MPP sequence

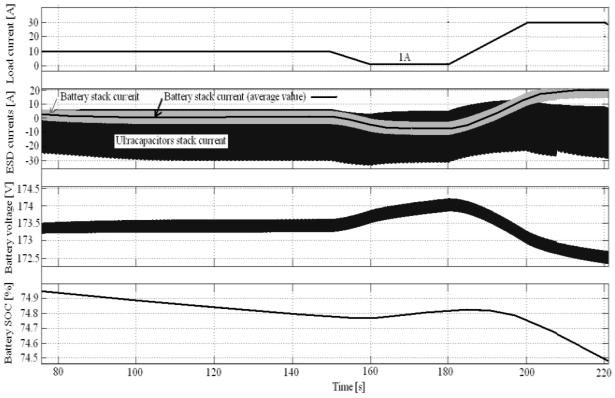

Figure 10. The HPS behaviour under a set load sequence

VI. CONCLUSIONS

In this paper, the control objective for the fuel cell HPS is to operate at the MPP of PEMFC for any dynamic of load. The proposed HPS architecture was modelled in Matlab–Simulink® environment. The simulation results have successfully shown that this operation of HPS is possible by using an adaptive MPP tracking control. The power balance is assured by the ESD stack.

REFERENCES

[1] NETL, "NETL Published Fuel Cell Specifications", accessed in 2 may 2010 on http://www.netl.doe.gov.

[2] C. Woojin, J. Gyubum, N.E. Prasad and W.H. Jo, "An Experimental Evaluation of the Effects of Ripple Current Generated by the Power Conditioning Stage on a Proton Exchange Membrane Fuel Cell Stack", JMEPEG 13, pp. 257-264, 2004.

[3] C. Liu and J.S. Lai, "Low Frequency Current Ripple Reduction Technique with Active Control in a Fuel Cell Power System with Inverter Load", PESC'05, Vol. IEEE 36th, pp. 2905-2911, 2005.

[4] S. Wajiha, A.K. Rahul and M. Arefeen, "Analysis and Minimization of Input Ripple Current in PWM Inverters for Designing Reliable Fuel Cell Power Systems", Journal of Power Sources, 156, pp. 448-454, 2006.

[5] B. Choi, D. Kim, D. Lee, S. Choi and J. Sun, "Analyze on Input Filter Interaction in Switching Power Converter", IEEE Transaction on Power Electronics, 22 (2), pp. 452-460, 2007.

[6] G. Fontes, C. Turpin, S. Astier and T.A. Meynard, "Interactions between Fuel Cells and Power Converters: Influence of Current Harmonics on a Fuel Cell Stack", IEEE Trans. on Power Electronics, 22 (2), pp. 670-678, 2007.

[7] W. Schmittinger and A. Vahidi," A Review of the Main Parameters Influencing Long-Term Performance and Durability of PEM Fuel Cells", Journal of Power Sources, 180, pp. 1-4, 2008.

[8] P. Thounthong, B. Davat, S. Rael and P. Sethakul, "An Overview of Power Converters for a Clean Energy Conversion Technology", IEEE Industrial Electronics magazine, 3 (1), pp. 32-46, 2009.

[9] M. Marchestoni and C. Vacca, "New DC-DC Converter for Energy Storage System Interfacing in Fuel Cell Hybrid Electric Vehicles", IEEE Trans. on Power Electronics, 22 (1), pp. 301-308, 2007.

[10] C. Liu and J.S. Lai, "Low Frequency Current Ripple Reduction Tech. with Active Control in a Fuel Cell Power System with Inverter Load", IEEE Trans. on Power Electronics, 22 (4), pp. 1453-1463, 2007.

[11] H. Farzanehfard, et al., "A Bidirectional Soft Switched Ultracapacitor Interface Circuit for Hybrid Electric Vehicles", Energy Conversion and Management, 49, pp. 3578-3584, 2008.

[12] J.C. Hwang, L.H. Chen and S.N. Yeh, "Comprehensive Analysis and Design of Multi-Leg Fuel Cell Boost Converter", Applied Energy, 84, pp. 1274-1288, 2007.

[13] A. Yilanci, I. Dincer and H.K. Ozturk, "A Review on Solar-Hydrogen/Fuel Cell Hybrid Energy Systems for Stationary Applications", Progress in Energy and Combustion Science, 35, pp. 231-244, 2009.

[14] P. Nema, et al., "A Current and Future State of Art Development of Hybrid Energy System using Wind and PV-Solar: A Review", Renewable and Sustainable Energy Reviews, 13 (8), pp. 2096-2103, 2009.

[15] M. Uzunoglu and M.S. Alam, "Dynamic Modeling, Design, and Simulation of a Combined PEM Fuel Cell and Ultracapacitor System for Standalone Residential Applications", IEEE Trans. on Energy Conversion, 21, pp. 767-775, 2006.

[16] L. Xu, J. Li, J. Hua, X. Li and M. Ouyang, "Adaptive Supervisory Control Strategy of a Fuel Cell/Battery-Powered City Bus", Journal of Power Sources, 194, pp. 360-368, 2009.

[17] P. Thounthong and B. Davat, "A PEM Fuel Cell Power Source for Electric Vehicle Applications with Supercapacitor or Battery as Auxiliary", Progress in Fuel Cell Research, NY: Nova, 2007.

[18] S.M. Lukic, J. Cao, R.C. Bansal, F. Rodriguez and A. Emadi, "Energy Storage Systems for Automotive Applications", IEEE Trans. on Ind. Electron, 55, pp. 2258-2267, 2008.

[19] M.J. Kim and H. Peng, "Power Management and Design Optimization of Fuel Cell/Battery Hybrid Vehicles", Journal of Power Sources, 165, pp. 819-832, 2007.

[20] Y. Tang, W. Yuan, M. Pan, Z. Li, G. Chen and Y. Li, "Experimental Investigation of Dynamic Performance

and Transient Responses of a kW-Class PEM Fuel Cell Stack under Various Load Changes", Applied Energy, 87, pp. 1410-1417, 2010.
[21] N. Bizon, "Hybrid Power Source for Vehicle Applications Operating at Maximum Power Point of Fuel Cell Stack", Int. Conf. on Applied Electronics, APPEL'10, ISSN: 1803-7232, ISBN: 978-1-4244-6818-8, INSPEC: 11579461, pp. 3-10, 2010.
[22] G. de Cesare, D. Caputo and A. Nascetti, "Maximum Power Point Tracker for Portable Photovoltaic Systems with Resistive-Like Load", Solar Energy, 80, pp. 982-988, 2009.
[23] T. Tafticht, M.L. Doumbia and A. Cheriti, "An Improved Maximum Power Point Tracking Method for Photovoltaic Systems", Renewable Energy, 33, pp. 1508-1516, 2008.
[24] B.J. Huang, F.S. Sun and R.W. Ho, "Near-Maximum-Power-Point-Operation (nMPPO) Design of Photovoltaic Power Generation System", Solar Energy, 80, pp. 1003-1020, 2006.
[25] I. Munteanu, A.I. Bratcu and E. Changa, "Wind Turbulence used as Searching Signal for MPPT in Variable-Speed Wind Energy Conversion Systems", Renewable Energy, 34, pp. 322-327, 2009.
[26] Z.D. Zhong, et al., "Adaptive Maximum Power Point Tracking Control of Fuel Cell Power Plants", Journal of Power Sources, 176, pp. 259-269, 2008.
[27] R.N. Methekar, S.C. Patwardhan, R.D. Gudi and V. Prasad, "Adaptive Peak Seeking Control of a Proton Exchange Membrane Fuel Cell", Journal of Process Control, 20, pp. 73-82, 2010.
[28] S.K. Mazumder, R.K. Burra and K. Acharya, "A Ripple-Mitigating and Energy-Efficient Fuel Cell Power-Conditioning System", IEEE Transactions on Power Electronics, 22 (4), pp. 1429-1436, 2007.
[29] R.M. James , et al., "Analysis of Stationary Fuel Cell Dynamic Ramping Capabilities and Ultracapacitor Energy Storage using High Resolution Demand Data", Journal of Power Sources, 156, pp. 472-479, 2006.
[30] D. Feroldi , et al., "Energy Management Strategies based on Efficiency Map for Fuel Cell Hybrid Vehicles", Journal of Power Sources, doi: 10.1016/j, Journal of Power Sources, 01.040, 2009.
[31] Y. Tang, W. Yuan, M. Pan, Z. Li, G. Chen and Y. Li, "Experimental Investigation of Dynamic Performance and Transient Responses of a kW-Class PEM Fuel Cell Stack under Various Load Changes", Applied Energy, 87 (4), pp. 1410-1417, 2010.
[32] W.H. Zhu, R.U. Payne, D.R. Cahela and B.J. Tatarchuk, "Uniformity Analysis at MEA and Stack Levels for a Nexa PEM Fuel Cell System", Journal of Power Sources, 128, pp. 231-8, 2004.
[33] B. Gou, W.K. Na and B. Diong, "Fuel Cells: Modeling, Control, and Applications", CRC Press, Chapter 6, 2010.
[34] C. Kunusch, et al., "Characterization and Experimental Results in PEM Fuel Cell Electrical Behaviour", International Journal of Hydrogen Energy, doi:10.1016/j.ijhydene, 12, 123, 2009.
[35] M.V. Marcos and E.S. Gisele, "A Practical Model for Evaluating the Performance of Proton Exchange Membrane Fuel Cells", Renewable Energy, 34, pp. 1734-1741, 2009.
[36] O. Erdinc, B. Vural and M. Uzunoglu, "A Wavelet Fuzzy Logic based Energy Management Strategy for a Fuel Cell/Battery/Ultra-Capacitor Hybrid Vehicular Power System", Journal of Power Sources, 194 (1), pp. 369-380, 2009.
[37] M.C. Kisacikoglua, M. Uzunoglua and M.S. Alam, "Load Sharing using Fuzzy Logic Control in a Fuel Cell/Ultracapacitor Hybrid Vehicle", International Journal of Hydrogen Energy, 34, pp. 1497-1507, 2009.
[38] O. Tremblay, L.A. Dessaint and A.I. Dekkiche, "A Generic Battery Model for the Dynamic Simulation of Hybrid Electric Vehicles", Vehicle Power and Propulsion Conf., VPPC 2007, IEEE, pp. 284-289, 9-12 Sept. 2007.
[39] N. Bizon, "On Tracking Robustness in Adaptive Extremum Seeking Control of the Fuel Cell Power Plants", Applied Energy, 87, pp. 3115-3130, 2010.
[40] N. Bizon, "Optimal Filtering of the Fuel Cell Power Probing Signal for Maximum Power Point Robust Adaptive Tracking", Int. Conf. on Applied Electronics APPEL'10, ISSN: 1803-7232, ISBN: 978-1-4244-6818-8, INSPEC: 11579510, pp. 43-46, 2010.

BIOGRAPHY

Nicu Bizon was born in Albesti Muscel, Romania, on February 14, 1961. He received a five-year degree in electronic engineering from the University "Polytechnic" of Bucharest, Romania, in 1986 and the Ph.D. degree in Automatic Systems and Control from the same university, in 1996. He is currently a Professor with the University of Pitesti, Romania. Previously, he was in hardware design with Dacia Renault SA, Romania.
He has authored of six books in Power Converter area, one in Theory and Control Systems, one in Fuzzy Control, one in Hardware topologies for PC and Devices, and one in Medical Electronics and Informatics (all in Romanian language). Also, he is co-authored of the book Fundamentals of Electromagnetic Compatibility, Theory and Practice (in English language) and of a book chapter - "Intelligent control of the Energy Generation System", in the book "Intelligent Information Systems and Knowledge Management for Energy: Applications for Decision Support, Usage and Environmental Protection". His current research interests include the broad area of nonlinear systems, on both dynamics and control, and power electronics. He has authored or coauthored of several papers (over to 100) in journals (ISI/INSPEC or Romanian Academy indexed) and international conference proceedings. He is an Associate Editor of Scientific journal of the University of Pitesti "Electronics and Computer Science" and program chair and proceeding Editor of the Int. Conference on "Electronics, Computers and Artificial Intelligence - ECAI", 2005, 2007 and 2009 editions.